

A Piecewise Linear Approach Towards Sheet Control in a Printer Paper Path

Björn Bukkems, René van de Molengraft, Maurice Heemels, Nathan van de Wouw and Maarten Steinbuch

Abstract—In this paper an approach towards sheet control in a printer paper path is presented. To make the control problem feasible, the complex overall control question is formulated in a hierarchical control set-up with a low level motor control part and a high level sheet control part. To understand the essence of the sheet control problem we consider a basic paper path in which industrial constraints and requirements are relaxed. Furthermore, the motor control part is assumed to be ideal and the sheet dynamics are captured in the piecewise linear modeling formalism. Based on the model of the sheet dynamics, the controller synthesis is carried out. Both state and output feedback control designs are presented and stability and tracking performance are analyzed. The effectiveness of the control design approaches is demonstrated via simulations.

I. INTRODUCTION

In this paper we consider longitudinal sheet handling in a cut sheet printer paper path. An example of such a paper path is shown in Fig. 1. Sheets enter the paper path at the Paper Input Module (PIM) and are transported to the Image Transfer Station (ITS) pinch where the image is printed onto the sheet at high pressure and high temperature. After leaving the ITS, sheets can either re-enter the first part of the paper path for back side printing or they can go to the finisher (FIN), where they are collected. The sheets are driven by pinches, which are sets of rollers that are, either individually or grouped together in sections, driven by motors.

One of the objectives of a printer's sheet handling mechanism is to accurately deliver sheets to the ITS. Each sheet must synchronize with its corresponding image with respect to both time and velocity to achieve a high printing quality. Whereas formerly printers were predominantly controlled in an open-loop fashion, nowadays feedback control is required to achieve the desired performance [1], [2], [3].

In the design of feedback control, dynamic paper path models are often used. In [1], [2] the paper path model is split up into two parts: the Section dynamics and the Sheet dynamics. The Section dynamics map the motor currents to section velocities, so these dynamics are essentially integrators. The Sheet dynamics, on the other hand, consist of

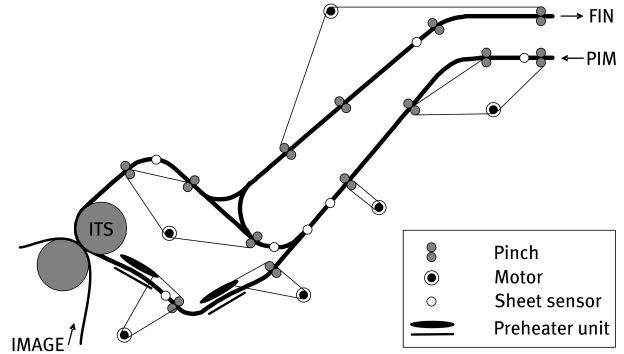


Fig. 1. Schematic representation of a printer paper path.

switching integrators. [1], [2] use a finite state machine to describe the discrete switching of a sheet between different sections: when entering a new section, the sheet velocity is suddenly dictated by the velocity of that section. The map from sheet velocities to sheet positions is described by integrators. The combination of the finite state machine and the integrators results in a hybrid dynamic model. On the basis of this model, a distributed, hybrid hierarchical control strategy is adopted, which controls the spacings between the sheets. The control design in [1], [2] is done intuitively and verified by simulation. A disadvantage of the control strategy used is the lack of analysis and systematic design methods, which makes it hard to prove the controller works under all conditions.

In this paper we present a more structured approach towards sheet control in a printer paper path that includes model-based control design, as well as stability and tracking performance analysis. To make the sheet control problem feasible we split up the control design in a motor control part and a sheet control part. As [1], [2], we recognize the state-dependent switching behavior of the Sheet dynamics. However, we capture these dynamics in the piecewise linear (PWL) modeling formalism [4]. The benefit of choosing this formalism is the availability of techniques for both controller synthesis and analysis, see for example [5], [6], [7], and the references therein. Regarding control design, we will exploit two different approaches. The first one covers a state feedback control design whereas in the second approach output feedback controllers are designed using loopshaping techniques [8]. Most literature on the analysis of piecewise linear control systems is devoted to stability analysis of the system dynamics. However, since we are dealing with a tracking problem, we will formulate the system in terms of

This work has been carried out as part of the Boderc project under the responsibility of the Embedded Systems Institute. This project is partially supported by the Netherlands Ministry of Economic Affairs under the Senter TS program.

Björn Bukkems, René van de Molengraft, Nathan van de Wouw and Maarten Steinbuch are with the department of Mechanical Engineering, Dynamics and Control Technology, Technische Universiteit Eindhoven, P.O. Box 513, 5600 MB Eindhoven, The Netherlands. {b.h.m.bukkems, m.j.g.v.d.molengraft, n.v.d.wouw, m.steinbuch}@tue.nl

Maurice Heemels is with the Embedded Systems Institute, P.O. Box 513, 5600 MB Eindhoven, The Netherlands. maurice.heemels@esi.nl

its error dynamics. By analyzing the stability of these error dynamics we can predict the tracking performance of the system at hand.

The remainder of this paper is organized as follows: in Section II the system under consideration will be discussed in more detail and the problem statement will be given, together with the control goal. In Section III we will discuss the two control design approaches. For both approaches, analysis on stability and performance will be given. In Section IV, simulation results will be shown, whereas in Section V the obtained results will be discussed in a broader context. Conclusions will come at the end.

II. SYSTEM OVERVIEW AND PROBLEM STATEMENT

When we consider sheet control in a printer paper path as the one shown in Fig. 1, we observe that the control design is complicated by industrial constraints and requirements. An example of such a constraint is that often several pinches are coupled and driven by the same motor. When there are two sheets in such a section, no independent sheet control is possible: adjusting the motor motion to counteract a position error of one sheet automatically implies the same change in profile for the other sheet. Another constraint arises when a sheet is in two sections at the same time, each driven by its own motor. To avoid buckling or tearing of the sheet, both sections must have approximately the same velocity. A requirement that challenges the control design is, for example, the desired high printing quality. Limited stiffness of paper path units, e.g. flexibilities in the driving belt between motors and pinches, will limit the attainable control performance. Consequently, it is not trivial how to achieve the desired quality.

To understand the core of the sheet control problem, we consider a basic version of a printer paper path. As a result, the fundamental parts of the control design naturally arise and a structured design approach can be more easily carried out. Therefore, we introduce the basic paper path depicted in Fig. 2. Since we consider the sheets only when they are in the paper path, the PIM and FIN are not taken into account. Furthermore, the loop is removed, so sheets cannot re-enter the path. The considered paper path consists of three pinches ($P1$, $P2$, and $P3$) only, each of which is driven by a separate motor ($M1$, $M2$, and $M3$, respectively). The locations of the three pinches in the paper path are represented by x_{P1} , x_{P2} , and x_{P3} , respectively. These locations are chosen such that

the distance between two pinches is equal to the sheet length L_s , so at each time instant the sheet is only in one pinch. No slip is assumed between the sheet and the pinches and the coupling between the pinches and motors is assumed to be infinitely stiff. The mass of the sheet is assumed to be zero, which simplifies modeling of the sheet dynamics. The sheet position, defined as x_s , is assumed to be measured. As optical sensors, like the ones used in optical mouse devices, are really cheap nowadays, this position measurement is becoming a serious option in printer control design. Despite this, an observer in combination with sheet sensors like the ones in the paper path in Fig. 1 may be a more practical solution.

As [1], [2], we also split up the complete sheet handling control problem into two levels. The low level encompasses motor modeling and control design, whereas on the high level the focus is on modeling and control of the sheet flow. The motor control is used to tackle disturbances and uncertainties at the motor level, e.g. friction in the bearings and flexibilities in the driving belt between motor and pinch. By introducing feedback at the high sheet level, robustness is obtained for disturbances and uncertainties on the sheet level. One can think of, for example, varying sheet characteristics related to geometry or roughness, tolerances on pinch radii and pinch positions, or slip between the sheet and pinches. Breaking up the control problem into two parts therefore seems natural for the system at hand and replaces the complex overall design question by two much simpler control questions. In this way, a cascade control structure is obtained in which the inner loop (the low level motor control loop) is designed to have a higher bandwidth than the outer loop (the high level sheet control loop) [9]. As a result the inner loop will closely track the reference profiles generated by the outer loop.

For the sheet motion task there are several possibilities, for example absolute reference tracking control and intersheet spacing control [1], [2]. In this paper we choose a constant velocity that has to be tracked by each individual sheet throughout the entire paper path. The corresponding sheet position setpoint $x_{s,r}$ will therefore be a first order ramp function. The control goal we adopt for the basic paper path case study is, given low level closed-loop systems and a high level sheet model, the design of high level feedback controllers (HLCs). These HLCs should result in stability of the high level closed-loop system and in a good tracking behavior of the sheet reference profile.

The low level motor control can be designed on the basis of standard single-input single-output motion control techniques [8]. The closed-loop linear motor dynamics in the Laplace domain can be represented by

$$\Omega_{Mi}(s) = T_i(s)\Omega_{Mi,r}(s), i \in \mathcal{I}, \quad (1)$$

with $T_i(s)$ the complementary sensitivity function of controlled motor i , which maps the input of the low level closed-loop system (the motor reference velocity $\omega_{Mi,r}(t)$, with $\omega_{Mi,r}(t)$ the inverse Laplace transform of $\Omega_{Mi,r}(s)$), to its output (the actual motor velocity $\omega_{Mi}(t)$). Furthermore, $\mathcal{I} = \{1, 2, 3\}$ represents the index set of sheet regions. To make

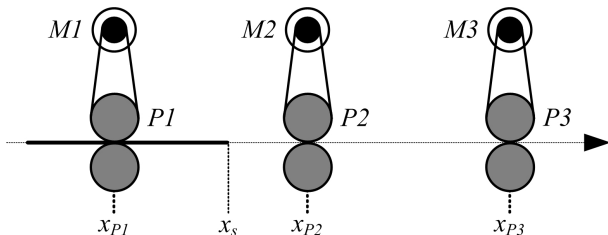


Fig. 2. Schematic representation of the simplified printer paper path.

the control problem even more feasible, we assume perfect tracking behavior of the controlled motors, i.e., $T_i(s) = 1$ in (1).

At the high level, modeling and control of the sheet dynamics are considered. Due to the assumption on ideal behavior in the low level control loop, the inputs u_i of the high level sheet dynamics will be directly calculated by the HLCs. This is shown in Fig. 3, which represents the block diagram of the control system at hand. Since at each time instant the sheet is only driven by one pinch, only one of the inputs of the high level sheet dynamics is used to calculate the sheet position. As the sheet moves through the paper path, this input will change when the sheet arrives at the next pinch. This switching behavior can be easily captured in the PWL modeling formalism. The sheet velocity is derived from the motor velocities via straightforward holonomic kinematic constraint relations that describe the relation between motor velocity and pinch velocity, and pinch velocity and sheet velocity, respectively. These constraint relations hold under the assumption that the connection between motor and pinch is infinitely stiff and that there is no slip between the pinch and the sheet. The sheet velocity is integrated to obtain the sheet position. The high level sheet model now becomes:

$$\dot{x}_s = B_i \underline{u} \quad \text{for } x_s \in \mathcal{X}_i, i \in \mathcal{I}, \quad (2)$$

with the input matrices B_i defined as $B_1 = [n_1 r_{P1} \ 0 \ 0]$, $B_2 = [0 \ n_2 r_{P2} \ 0]$, and $B_3 = [0 \ 0 \ n_3 r_{P3}]$, respectively. In these definitions, n_i represents the transmission ratio between motor i and pinch i and r_{Pi} represents the radius of pinch i . Furthermore, $\underline{u} = [u_1 \ u_2 \ u_3]^T$, $\mathcal{X}_1 = \{x_s | x_s \in [x_{P1}, x_{P2}]\}$, $\mathcal{X}_2 = \{x_s | x_s \in [x_{P2}, x_{P3}]\}$, and $\mathcal{X}_3 = \{x_s | x_s \in [x_{P3}, x_{P3} + L_s]\}$.

III. HIGH LEVEL CONTROL DESIGN

In this section we present two feedback control design approaches. Although in practical situations also a feed-forward control input will be used to achieve the desired tracking performance, the approaches presented here will focus only on feedback design. In the first approach, both the stability analysis and the state-feedback controller synthesis can be expressed as a convex optimization problem based on constraints in the form of a set of linear matrix inequalities (LMIs). Since we will base our analysis on the tracking error dynamics, stability will be directly linked to tracking performance. The second approach encompasses output feedback control design. Here, the HLCs will be designed

using loopshaping techniques based on the high level sheet model (2). After designing the controllers, the tracking error dynamics will be derived and the stability of these dynamics will be analyzed by solving a set of LMIs.

A. STATE FEEDBACK CONTROL DESIGN

To formulate the error dynamics for the high level sheet dynamics (2), we use the error-space approach of [8] and extend it to the PWL case. Since the sheet reference profile is assumed to be of first order, it will have zero acceleration:

$$\ddot{x}_{s,r} = 0. \quad (3)$$

The sheet tracking error is defined as the difference between the sheet reference position and the actual sheet position:

$$e_s = x_{s,r} - x_s. \quad (4)$$

Substitution of (3) in the second derivative of (4) yields

$$\ddot{e}_s = -\ddot{x}_s. \quad (5)$$

We now define error-space state ξ as:

$$\xi = \ddot{x}_s. \quad (6)$$

With this definition, (5) becomes

$$\ddot{e}_s = -\xi. \quad (7)$$

Next, the control input \underline{u} is replaced by the control input in error-space, which is defined as:

$$\underline{\mu} = \underline{\ddot{u}}. \quad (8)$$

With these definitions, the state equation for the error-space state ξ now becomes:

$$\begin{aligned} \dot{\xi} &= \ddot{x}_s \\ &= B_i \underline{\mu} \quad \text{for } x_s \in \mathcal{X}_i, i \in \mathcal{I}. \end{aligned} \quad (9)$$

The expressions (7) and (9) now describe the overall system in the error-space. In standard state-variable form, the error dynamics now become:

$$\dot{\underline{q}} = F \underline{q} + G_i \underline{\mu} \quad \text{for } x_{s,r} - [1 \ 0 \ 0] \underline{q} \in \mathcal{X}_i, i \in \mathcal{I}, \quad (10)$$

with $\underline{q} = [e_s \ \dot{e}_s \ \xi]^T$ the state vector of the error dy-

namics. The matrices $F = \begin{bmatrix} 0 & 1 & 0 \\ 0 & 0 & -1 \\ 0 & 0 & 0 \end{bmatrix}$ and $G_i =$

$[0_{3 \times 1} \ 0_{3 \times 1} \ B_i^T]^T$ represent the state and input matrices of the error dynamics, respectively.

Given these error dynamics, the goal is to find a control law that stabilizes these dynamics. This control law should result in regulation of the error dynamics, i.e. all error states should go to zero. This automatically implies that the actual sheet position will become equal to the desired one and, hence, the desired tracking performance will be obtained. The control law we propose is based on state feedback:

$$\underline{\mu} = -K_S \underline{q}, \quad (11)$$

with K_S the matrix with state feedback gains. Elimination of $\underline{\mu}$ in (8) by substitution of (11) and integrating twice

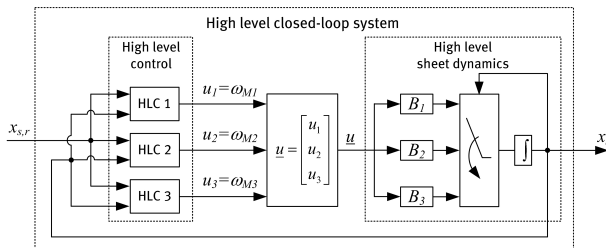


Fig. 3. Block diagram of the total control system.

yields the control law for each region for the high level sheet model (2):

$$\begin{aligned} u_i = & -K_{S,i}(3)x_s - K_{S,i}(2) \int_{t_0}^t e_s d\tau - \\ & -K_{S,i}(1) \int_{t_0}^t \int_{t_0}^\zeta e_s d\tau d\zeta \\ & \text{for } x_{s,r} - \begin{bmatrix} 1 & 0 & 0 \end{bmatrix} \underline{q} \in \mathcal{X}_i, i \in \mathcal{I}, \end{aligned} \quad (12)$$

with t_0 the initial time and $K_{S,i}(j)$ the j -th element of the i -th row of K_S , $i \in \mathcal{I}$, $j \in \{1, 2, 3\}$.

To analyze the stability of the error dynamics and to calculate the controller gains, first (11) is substituted into (10), yielding the following closed loop error dynamics:

$$\dot{\underline{q}} = (F - G_i K_S) \underline{q} \quad \text{for } x_{s,r} - \begin{bmatrix} 1 & 0 & 0 \end{bmatrix} \underline{q} \in \mathcal{X}_i, i \in \mathcal{I}. \quad (13)$$

By making use of the work presented in [10], it can be analyzed whether the closed-loop error dynamics in (13) is Globally Exponentially Stable (GES). To do so, we propose a common quadratic Lyapunov function candidate:

$$V(\underline{q}) = \underline{q}^T P \underline{q}, \quad (14)$$

with $P = P^T > 0$. To prove that the error dynamics is GES, the following set of matrix inequalities in P and K_S must hold:

$$\begin{aligned} 0 & \geq \dot{V}(\underline{q}) + \alpha V(\underline{q}) \\ 0 & \geq (F - G_i K_S)^T P + P(F - G_i K_S) + \alpha P, i \in \mathcal{I}, \end{aligned} \quad (15)$$

where $\alpha > 0$ represents the decay rate of the Lyapunov function. This parameter is chosen a priori in relation to the desired tracking performance. A large value of α results in a fast convergence of the error to zero. When α is chosen too large, (15) does not have a feasible solution. From (15), it becomes clear that both the stability analysis and the calculation of the controller gains can be carried out by solving the set of matrix inequalities. Since these matrix inequalities are not linear in the unknown matrices P and K_S , we pre and post-multiply (15) with P^{-1} and substitute $Q = P^{-1}$ and $Y = K_S P^{-1}$ to obtain the following set of LMIs in Q and Y :

$$\begin{aligned} 0 & \geq FQ + QF^T - G_i Y - Y^T G_i^T + \alpha Q, i \in \mathcal{I} \\ 0 & < Q. \end{aligned} \quad (16)$$

After solving these LMIs, the controller gains can be calculated using

$$K_S = YQ^{-1}. \quad (17)$$

B. OUTPUT FEEDBACK CONTROL DESIGN

The output feedback control design approach follows a different strategy than the state feedback design method. In this case we start with the design of three HLCs for the three subsystems of the high level sheet model (2). The design procedure makes use of loopshaping techniques [8]. Since each subsystem $H_i(s)$ consists of an integrator multiplied by a gain:

$$H_i(s) = \frac{n_i r_{Pi}}{s}, i \in \mathcal{I}, \quad (18)$$

and the sheet reference profile is a ramp function, we propose a Proportional-Integral (PI) controller for each subsystem:

$$\begin{aligned} C_i(s) &= \frac{U_i(s)}{E_s(s)} \\ &= \frac{P_i s + I_i}{s}, i \in \mathcal{I}. \end{aligned} \quad (19)$$

The controller gains P_i and I_i are tuned such that the desired bandwidth is obtained. Given this PI controller and a ramp-shape reference profile, we enforce a zero tracking error in each subsystem for $t \rightarrow \infty$. This can be shown using the Final Value Theorem [8]:

$$\lim_{t \rightarrow \infty} e_s(t) = \lim_{s \rightarrow 0} s E_s(s). \quad (20)$$

In (20), $E_s(s)$ is the Laplace transform of $e_s(t)$, calculated from the sensitivity function $S_i(s)$:

$$\begin{aligned} S_i(s) &= \frac{E_s(s)}{X_{s,r}(s)} \\ &= \frac{1}{1 + H_i(s)C_i(s)} \\ &= \frac{s^2}{s^2 + P_i n_i r_{Pi} s + I_i n_i r_{Pi}}, i \in \mathcal{I} \end{aligned} \quad (21)$$

with $X_{s,r}(s)$ representing the Laplace transform of the sheet reference position $x_{s,r}(t)$. Substitution of (21) into (20) yields the desired proof for tracking performance of each individual subsystem.

However, this does not guarantee stability for the high level error dynamics, due to the switching behavior. To analyze this stability, we write the control law (19) in the time domain and differentiate twice with respect to time:

$$\ddot{u}_i = P_i \ddot{e}_s + I_i \dot{e}_s, i \in \mathcal{I}. \quad (22)$$

Combining (22), (7), and (8) yields the following control input in the error-space:

$$\begin{aligned} \mu_i &= -P_i \xi + I_i \dot{e}_s \\ &= K_{L,i} \underline{q}, i \in \mathcal{I}, \end{aligned} \quad (23)$$

with $K_{L,i} = [0 \ I_i \ -P_i]$ the i -th row of the matrix K_L with output feedback gains. Substitution of (23) in (10) yields the closed-loop error dynamics:

$$\dot{\underline{q}} = (F + G_i K_L) \underline{q} \quad \text{for } x_{s,r} - \begin{bmatrix} 1 & 0 & 0 \end{bmatrix} \underline{q} \in \mathcal{X}_i, i \in \mathcal{I}. \quad (24)$$

Using a similar approach as presented in Section III-A, the stability of the closed-loop error dynamics (24) can be analyzed. The objective in this case is, given $K_{L,i}$, to find a matrix $P = P^T > 0$ in the Lyapunov function candidate (14) that satisfies the following set of LMIs in P :

$$0 \geq (F + G_i K_L)^T P + P(F + G_i K_L) + \alpha P, i \in \mathcal{I}. \quad (25)$$

When the control laws of the two design approaches are compared it can be observed that the state feedback controller integrates the error twice, whereas in the output feedback case only one integrator is incorporated. In the latter case the loopgain contains two pure integrators, i.e. one from the high level sheet model and one from the controller, which was shown to be needed to obtain a zero tracking error. In the state feedback approach, the pure integrator in the sheet model becomes a first order filter due to the proportional state feedback term $-K_{S,i}(3)x_s$. Consequently, the error needs to be integrated twice to achieve the desired tracking performance.

IV. SIMULATION RESULTS

To demonstrate the effectiveness of the two control design approaches, simulations have been conducted for the basic paper path shown in Fig. 2. A letter-format sheet, of which the length is 0.216 m, enters the paper path at $t = 0.5$ s. It has to be transported at a velocity of 0.25 m/s and leaves the paper path when its trailing edge has left $P3$. The sheet reference profile is depicted in Fig. 4. The distance between the pinches is chosen to be equal to the sheet length: $x_{P1} = 0$ m, $x_{P1} = L_s$ m, and $x_{P3} = 2L_s$ m. Pinches with different radii are chosen to emphasize the piecewise linear character of the high level sheet model: $r_{P1} = 20 \cdot 10^{-3}$ m, $r_{P2} = 22 \cdot 10^{-3}$ m, $r_{P3} = 25 \cdot 10^{-3}$ m. The same has been done with the transmission ratios: $n_1 = \frac{1}{3}$, $n_2 = \frac{4}{9}$, and $n_3 = \frac{1}{2}$.

A. STATE FEEDBACK CONTROL RESULTS

Given the dimensions of the basic paper path we calculate the state feedback controller gains and verify the stability of the error dynamics by solving the set of LMIs given in (16). A positive definite, symmetric matrix P is found, which proves that the closed loop error dynamics (13) is GES. The chosen decay rate $\alpha = 50$ results in convergence of the tracking error to zero within 0.2 [s]. The controller gains $K_{S,i}$ to be used in the control law (12) are the following: $K_{S,1} = [-4.0 \cdot 10^7 \ -2.2 \cdot 10^6 \ 3.1 \cdot 10^4]$, $K_{S,2} = [-2.8 \cdot 10^7 \ -1.5 \cdot 10^6 \ 2.1 \cdot 10^4]$, and $K_{S,3} = [-2.2 \cdot 10^7 \ -1.2 \cdot 10^6 \ 1.7 \cdot 10^4]$. Given these controller gains, the sheet tracking error depicted in Fig. 5 is obtained. It can be seen that the sheet controller anticipates quickly to the initial error, which is due to the difference in actual and desired sheet velocity at $t = 0.5$ [s]. Furthermore, we notice that after the transient response the error stays zero, also at the switching planes.

To analyze the robustness of the controlled system to changes in the input gains B_i , the gains used in the control design have been slightly perturbed in the simulation. With respect to their original values, the actual gains vary 9%, -7%, and 8%, respectively. The tracking error obtained

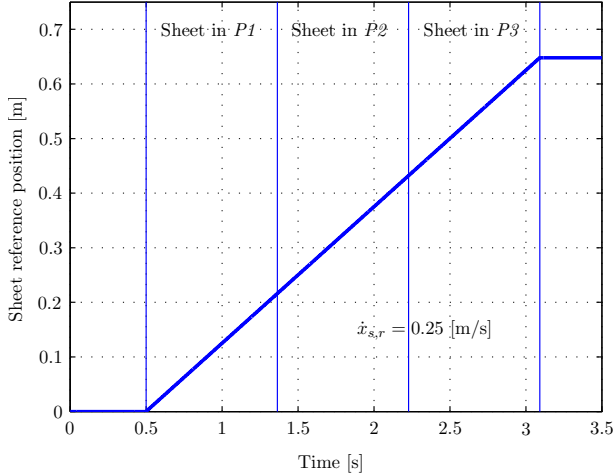


Fig. 4. Sheet position reference profile.

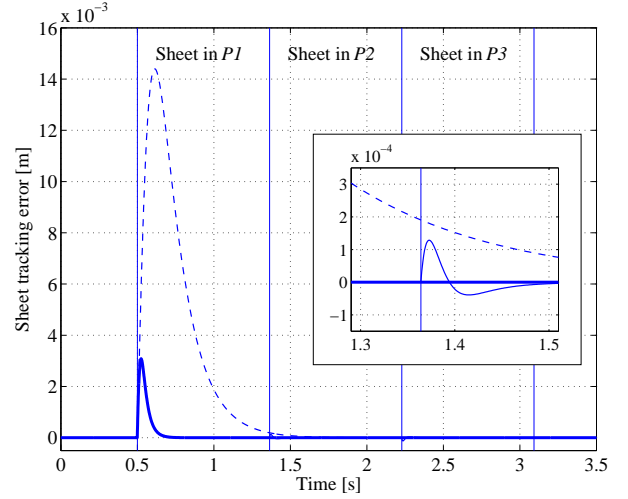


Fig. 5. State feedback control approach: tracking error without disturbances for $\alpha = 50$ (thick) and $\alpha = 10$ (dashed) and with perturbations for $\alpha = 50$ (thin).

using these perturbed gains is depicted in Fig. 5 as well. It can be seen that the maximum deviation from the desired zero error level after the switching moments is approximately $1.3 \cdot 10^{-4}$ m, which is well acceptable, and that these errors are controlled to zero fast.

Fig. 5 also shows the tracking error obtained without perturbing the input gains but with using controller gains resulting from setting $\alpha = 10$. These smaller controller gains result in a slower transient response and in a nonzero tracking error when transferring the sheet from $P1$ to $P2$. Also during this switch between regions the error is not amplified.

B. OUTPUT FEEDBACK CONTROL RESULTS

Also the output feedback controllers are tuned to achieve a fast convergence of the tracking error to zero. The controller gains P_i and I_i in (19) are chosen such that a crossover frequency is realized that is comparable to the one obtained with the state feedback control approach in case $\alpha = 50$. In Fig. 6 the frequency response functions of the loopgains of the first subsystem, obtained in both control approaches, are depicted. From this figure, it can be seen that the crossover frequency is approximately 11 Hz. By placing the zero of the controller (19) at 11 Hz, a phase margin of 45° is obtained, which results in robustness for model uncertainties.

The controller gains obtained in the output feedback control design are the following: $P_1 = 7.3 \cdot 10^3$, $I_1 = 5.0 \cdot 10^5$, $P_2 = 5.0 \cdot 10^3$, $I_2 = 3.4 \cdot 10^4$, and $P_3 = 3.9 \cdot 10^3$, $I_3 = 2.7 \cdot 10^4$. Using these controller gains, the set of LMIs in (25) is solved, yielding a positive definite, symmetric matrix P , which proves that the closed loop error dynamics (24) is GES. Also using this controller simulations have been carried out. The results obtained when the input gains B_i have been perturbed are shown in Fig. 7. As with the state feedback design approach, the initial error as well as the errors after the switching moments are quickly removed.

In both control design approaches, high controller gains can lead to high demands on actuators in the low level control loop. Therefore, in practical cases, care must be taken not

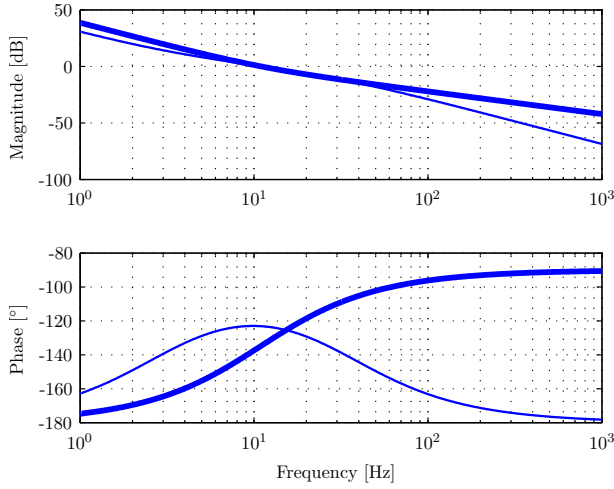


Fig. 6. Frequency response function of the loopgain of the first subsystem in the output feedback case (thick) and the state feedback case (thin).

to violate physical constraints, such as maximum allowable velocities and accelerations. Incorporating such constraints in the control design will be subject of future research.

V. DISCUSSION

In the sheet control case-study presented, two design approaches have been applied. In the state-feedback control design, both the stability analysis and the controller synthesis are performed by solving an optimization problem. This is a benefit over the output feedback control design approach, in which the stability has to be post-analyzed. A drawback, however, is that there is less insight in the tuning of the controller than in the loopshaping approach.

Besides the control design approaches presented in this paper, there are more possible design procedures, e.g., feedback linearization [11]. In order to achieve perfect linearization and, hence, a linear control problem, the system parameters must be exactly known. However, robustness against uncertainty and variations of these parameters was the main motivation for sheet feedback control in the first place.

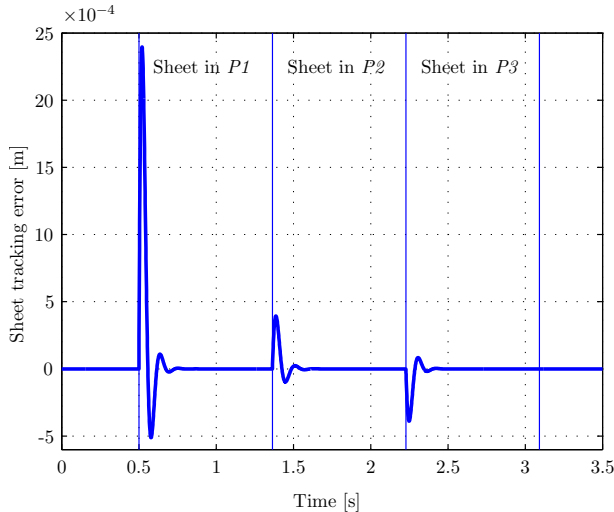


Fig. 7. Output feedback control approach: tracking error with perturbations.

VI. CONCLUSIONS

This paper presents an approach towards sheet control in a printer paper path. By introducing assumptions that relax some of the industrial constraints and requirements, and by splitting up the complex overall control design problem into a simple motor and sheet control design part, the core of the design question is exposed. As the inner loop of the resulting cascade control system, i.e., the motor control loop, is assumed to be perfect, the focus is on the design of feedback controllers for the remaining piecewise linear sheet dynamics. Controllers that result in stable error dynamics and good tracking performance have been proposed. In the case of state feedback control, both the controller synthesis as well as the stability analysis have been expressed as a convex optimization problem based on constraints in the form of a set of linear matrix inequalities. The output feedback control design has been carried out using loopshaping techniques, whereas the analysis of both stability and tracking performance have been carried out by solving a set of linear matrix inequalities a posteriori. Simulation results confirm the good tracking performance and show robustness against varying system parameters. Since industrial printer paper paths are far more complex than the one used in this paper, future research will gradually release the simplifying assumptions made in this paper. Topics for investigation will be, for example, control design for cases in which pinches are coupled into sections, driven by one motor, and cases in which more than one pinch can influence the sheet motion.

VII. ACKNOWLEDGMENTS

The authors gratefully acknowledge the contribution of Jeroen de Best for his input on the derivation of the closed-loop error dynamics in Section III-A.

REFERENCES

- [1] M. Kruciński, *Feedback Control of Photocopying Machinery*, Ph.D. thesis, University of California Berkeley, CA, USA, 2000.
- [2] C. Cloet, *A Mechatronics Approach to Copier Paperpath Design*, Ph.D. thesis, University of California Berkeley, CA, USA, 2001.
- [3] S. Rai and W. B. Jackson, "A hybrid hierarchical control architecture for paper transport systems," in *Proc. of the 37th IEEE Conference on Decision and Control*, Tampa, Florida, USA, December 1998, pp. 4249–4250.
- [4] E. D. Sontag, "Nonlinear regulation: The piecewise linear approach," *IEEE Trans. Automat. Contr.*, vol. 26(2), pp. 346–381, April 1981.
- [5] M. Johansson and A. Rantzer, "Computation of piecewise quadratic lyapunov functions for hybrid systems," *IEEE Trans. Automat. Contr.*, vol. 43(4), pp. 555–559, April 1998.
- [6] A. Hassibi and S. Boyd, "Quadratic stabilization and control of piecewise-linear systems," in *Proc. of the American Control Conference*, Philadelphia, PA, USA, June 1998, pp. 3659–3664.
- [7] G. Feng, G. Lu, and S. Zhou, "An approach to H_∞ controller synthesis of piecewise linear systems," *Communications in Information and Systems*, vol. 2(3), pp. 245–254, December 2002.
- [8] G. F. Franklin, J. D. Powell, and A. Emami-Naeini, *Feedback control of dynamic systems*. Upper Saddle River, New Jersey, USA: Prentice Hall, 2002.
- [9] G. Stephanopoulos, *Chemical Process Control*. Englewood Cliffs, New Jersey, USA: Prentice Hall, 1984.
- [10] R. A. DeCarlo, M. S. Branicky, S. Pettersson, and B. Lennartson, "Perspectives and results on the stability and stabilizability of hybrid systems," *Proc. IEEE*, vol. 88(7), pp. 1069–1082, July 2000.
- [11] H. K. Khalil, *Nonlinear Systems*. Upper Saddle River, New Jersey, USA: Prentice Hall, 2002.